RESULTS ANALYSIS IN A CONSTRAINED REAL-TIME OPTIMIZATION (RTO) SYSTEM

W. S. Yip and T. E. Marlin

Department of Chemical Engineering, McMaster University, Hamilton, ON L8S 4L7, Canada

Abstract: This paper presents a new results analysis strategy for uncertain real-time optimization (RTO) systems. The key contributions of this paper are in 1) developing a mathematical formulation describing the confidence region of a partially constrained optimum and 2) applying that formulation in deciding whether the optimizer results should be implemented. The confidence region of the constrained optimum is determined from the confidence region of the unconstrained optimum, when the inequality constraints are not considered. The confidence region of the unconstrained optimum is mapped to the feasible region defined by the inequality constraints to obtain the confidence region of the constrained optimum. This mapping is developed by minimizing the profit loss between the unconstrained and constrained optima. The resulting confidence region of the constrained optimum is used in optimization results analysis; the confidence regions of successive predicted optima are compared to decide if the difference between two optima is statistically significant. The comparison is made by calculating the significance level at which the two confidence regions just overlap. If the value is small, large portions of two 95% confidence regions overlap, and the optimizer result will not be implemented. The new results analysis approach is applied to the Williams-Otto reactor case study with controlled inequality constraints, where it significantly reduced plant variability, while concurrently increasing the operating profit.

Keywords: Real-time optimisation, results analysis, constrained optimum

1. INTRODUCTION

Real-time operations optimization (RTO) can improve the operating profit of chemical plants by tracking the changing optimum due to disturbances such as changes in plant performance and external state variables. This paper focuses on the model-based real-time operations optimization using steady-state models, in which the RTO execution period is much longer than the feedback dynamics. In this situation, a steady-state model is sufficient for economic optimization.

The main elements in the RTO loop [Marlin and Hrymak, 1997] consist of the model updater, model-based optimizer, results analysis and process control as shown in Figure 1. Real-time measurements ($\mathbf{z}$) are taken from the plant, checked for reliability and low pass filtered. Then, the process parameters ($\boldsymbol{\beta}$) are estimated using the data in the model updater. The estimated parameters are then sent to the optimizer, in which model-based optimization is performed. The optimizer results are analyzed in results analysis [Miletic and Marlin, 1998] before being transmitted to the process controllers. Only significant changes in optimization variables are forwarded to the process controllers for implementation. The new setpoint can be determined by trading off the change in profit and the size of the change of the operating variables [Ronholm and Marlin, 2002] to make the transition more gradual.

The performance of an RTO system is measured by two terms: 1) *offset* between the plant optimum and noise-free model prediction, and 2) *variability* of the prediction. Offset is caused by the structural mismatch between the plant and the model and the errors in the parameter values. Variability is caused by high frequency disturbances and measurement noise propagating in the RTO loop. Offset and variability can have a significant impact on the operating profit, and a small offset and variability is desirable in profit tracking.

This paper focuses on improving the RTO performance by reducing the variability of the manipulated variables in a partially constrained RTO system. The RTO results are influenced by high frequency variation and should be evaluated with respect to the common cause variability. In results analysis [Miletic and Marlin, 1998], the newly predicted (uncertain) optimum is compared with the previous (uncertain) results in deciding whether the new result shall be implemented or not. In previous work, it was assumed that the active set of inequality constraints remains unchanged when the parameters are perturbed. Therefore, the covariance matrix of the predicted optimum can be estimated by linear sensitivity analysis and a statistical test can be formulated as a Hotelling T^2 test. In this paper, the assumption of a constant active set will be relaxed and a new strategy of results analysis will be developed to handle the possible change in the active set of inequality constraints.

The outline of this paper is as follows. The mathematical formulation to describe the confidence region of the constrained optimum is first developed. The new strategy of results analysis using the developed formulation for the uncertainty of the constrained optimum is then presented. Finally, the proposed approach is applied to the Williams-Otto reactor system to investigate if the results analysis can reduce the unnecessary plant movement responding to high frequency disturbances.

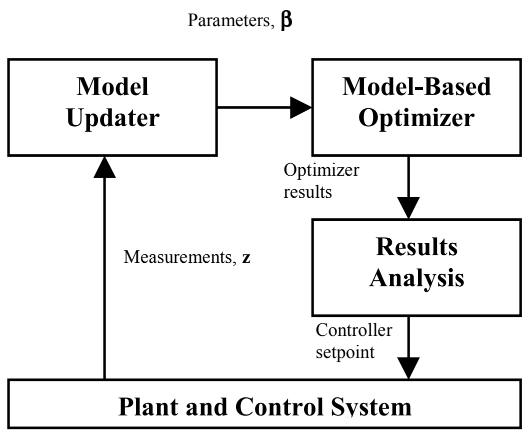

Fig. 1 Closed-loop RTO system

2. MATHEMATICAL FORMULATION FOR THE UNCERTAINTY OF THE CONSTRAINED OPTIMUM

In this section, the method to estimate the confidence region of the constrained optimum is presented. The optimization problem considered in this paper is formulated as follows

$$\underset{\mathbf{x},\,\mathbf{u}}{\text{Maximize}} \quad P(\mathbf{x}, \mathbf{u}, \boldsymbol{\beta}) \qquad (1)$$

$$\text{Subject to} \quad \mathbf{h}(\mathbf{x}, \mathbf{u}, \boldsymbol{\beta}) = \mathbf{0}$$
$$\mathbf{w}(\mathbf{x}, \mathbf{u}, \boldsymbol{\beta}) \le \mathbf{0}$$

where $\mathbf{x}$ is the vector of decision variables implemented to the plant, $\mathbf{u}$ is the vector of dependent variables, $\mathbf{h}$ and $\mathbf{w}$ are the equality and inequality constraints respectively and P is the objective function. The vector of parameters, $\boldsymbol{\beta}$, is estimated from the updater, and its uncertainty is described by the confidence region given in (2)

$$\left(\boldsymbol{\beta}-\hat{\boldsymbol{\beta}}\right)^T \mathbf{Q}_{\boldsymbol{\beta}}^{-1}\left(\boldsymbol{\beta}-\hat{\boldsymbol{\beta}}\right) \le \chi^2(\alpha, \nu_\beta) \qquad (2)$$

where $\hat{\boldsymbol{\beta}}$ is the nominal value of the estimated parameters, $\mathbf{Q}_\beta$ is the covariance matrix of the estimated parameters, χ^2 is the Chi-square distribution, α% is the level of confidence and ν_β is the degrees of freedom which is equal to the number of the estimated parameters, assuming the covariance matrix is known [Anderson, 1984]. In this work, a possible change in the active set of the inequality constraints, $\mathbf{w}$, may occur for the anticipated uncertainty of $\boldsymbol{\beta}$ given in (2).

The confidence region of the constrained optimum, $\mathbf{x}_c^*$, which is the solution of (1), is obtained by "mapping" the confidence region $\mathbf{x}_u^*$ to the region defined by the inequality constraints as shown in Figure 2. The unconstrained optimum, $\mathbf{x}_u^*$, is the solution of the following optimization problem, which is the original problem (1) without the inequality constraints.

$$\underset{\mathbf{x},\,\mathbf{u}}{\text{Maximize}} \quad P(\mathbf{x}, \mathbf{u}, \boldsymbol{\beta}) \qquad (3)$$

$$\text{Subject to} \quad \mathbf{h}(\mathbf{x}, \mathbf{u}, \boldsymbol{\beta}) = \mathbf{0}$$

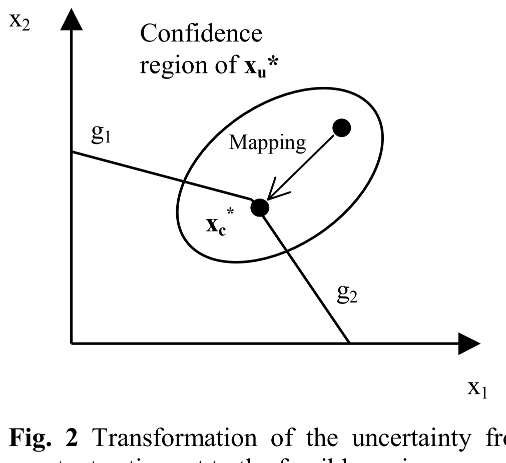

Fig. 2 Transformation of the uncertainty from the constant active set to the feasible region

The confidence region of $\mathbf{x}_u^*$ can be determined by linear sensitivity analysis [Fiacco, 1983] of problem (3) because the active set of inequality constraints remains constant. All linearizations are performed at the nominal value of the estimated parameter, $\hat{\boldsymbol{\beta}}$, and the unconstrained optimum, $\hat{\mathbf{x}}_\mathbf{u}^*$, estimated from $\hat{\boldsymbol{\beta}}$. The covariance matrix of $\mathbf{x}_u^*$ is given in (4).

$$\mathbf{Q}_{\mathbf{x}_u^*} = \left(\frac{d\mathbf{x}_\mathbf{u}^*}{d\boldsymbol{\beta}}\right)\mathbf{Q}_\beta\left(\frac{d\mathbf{x}_\mathbf{u}^*}{d\boldsymbol{\beta}}\right)^T \tag{4}$$

The procedure in calculating the sensitivity matrix $\frac{d\mathbf{x}_\mathbf{u}^*}{d\boldsymbol{\beta}}$ for problem (3) is discussed in Wolbert, et al. (1994). The confidence region of $\mathbf{x}_u^*$ is given in (5)

$$\left(\mathbf{x}_\mathbf{u}^* - \hat{\mathbf{x}}_\mathbf{u}^*\right)^T \mathbf{Q}_{\mathbf{x}_u^*}{}^{-1}\left(\mathbf{x}_\mathbf{u}^* - \hat{\mathbf{x}}_\mathbf{u}^*\right) \leq \chi^2(\alpha, \nu_X) \tag{5}$$

where ν_X is the degrees of freedom in (3) which is equal to the dimension of $\mathbf{x}$.

The confidence region of $\mathbf{x}_c^*$ can be derived by mapping every point inside the confidence region of $\mathbf{x}_u^*$ given in (5) to the feasible region defined by the inequality constraints in the reduced space. By eliminating $\mathbf{u}$ using $\mathbf{h}(\mathbf{x}, \mathbf{u}, \boldsymbol{\beta}) = \mathbf{0}$, Equation (1) can be written as follows

$$\underset{\mathbf{x}}{\text{Maximize}} \quad P_r(\mathbf{x}, \boldsymbol{\beta}) \tag{6}$$

Subject to $\mathbf{g}(\mathbf{x}, \boldsymbol{\beta}) \leq \mathbf{0}$

where P_r and $\mathbf{g}$ are the objective function and inequality constraints in the reduced space. The solution of (6) is exactly the same as $\mathbf{x}_c^*$ if we can analytically solve for $\mathbf{u}$ from $\mathbf{h}(\mathbf{x}, \mathbf{u}, \boldsymbol{\beta}) = \mathbf{0}$. If we must linearize $\mathbf{h}(\mathbf{x}, \mathbf{u}, \boldsymbol{\beta}) = \mathbf{0}$ to eliminate $\mathbf{u}$, Equation (6) is an approximation of (1).

As shown in Figure 2, the collection of the points after the mapping in the region bounded by $\mathbf{g}(\mathbf{x}, \boldsymbol{\beta}) \leq \mathbf{0}$ defines the confidence region of the constrained optimum. For a given value of $\boldsymbol{\beta}$ inside the confidence region defined in (2), the unconstrained optimum $\mathbf{x}_u^*$ can be estimated from the linear approximation as follows.

$$\mathbf{x}_\mathbf{u}^* - \hat{\mathbf{x}}_\mathbf{u}^* = \frac{d\mathbf{x}_\mathbf{u}^*}{d\boldsymbol{\beta}}\left(\boldsymbol{\beta} - \hat{\boldsymbol{\beta}}\right) \tag{7}$$

For every value of $\boldsymbol{\beta}$, the difference in profit at $\mathbf{x}_u^*$ and $\mathbf{x}_c^*$ should be minimum. Therefore, (6) can be expressed without changing the result [$P_r(\mathbf{x}_u^*, \boldsymbol{\beta})$ is a constant] as follows

$$\underset{\mathbf{x}}{\text{Minimize}} \; P_r(\mathbf{x}_u^*, \boldsymbol{\beta}) - P_r(\mathbf{x}, \boldsymbol{\beta}) \tag{8}$$

Subject to $\mathbf{g}(\mathbf{x}, \boldsymbol{\beta}) \leq \mathbf{0}$

and $\mathbf{x}_c^*$ is the optimum solution of (8). Furthermore, when $P_r(\mathbf{x}, \boldsymbol{\beta})$ can be approximated by expanding the profit function using Taylor's series around the point $\hat{\mathbf{x}}_u^*$, Equation (8) can be re-written as follows.

$$\underset{\mathbf{x}}{\text{Minimize}} - \left(\mathbf{x} - \mathbf{x}_\mathbf{u}^*\right)^T \nabla_r{}^2 P\Big|_{\hat{\mathbf{x}}_u^*}\left(\mathbf{x} - \mathbf{x}_\mathbf{u}^*\right) \tag{9}$$

Subject to $\mathbf{g}(\mathbf{x}, \boldsymbol{\beta}) \leq \mathbf{0}$

The reduced Hessian matrix can be obtained when calculating the sensitivity matrix in (4) using Wolbert's approach [1994]. For any point $\boldsymbol{\beta}$ sampled from the confidence region in (2), $\mathbf{x}_c^*$ can be estimated by solving (7) and (9). We can estimate the uncertain ranges of $\mathbf{x}_c^*$ by solving (7) and (9) for different values of $\boldsymbol{\beta}$ sampled from (2). If the inequality constraints are linear(ized), (9) becomes a quadratic programming (QP) problem that we can solve efficiently.

The confidence region obtained by solving (7) and (9) for a sample of $\boldsymbol{\beta}$ values is characterized by a collection of data points. In results analysis, it is difficult to evaluate two uncertain optimizer results from two sets of data points, since this is a bilevel optimization problem. Therefore, (9) is reformulated to a system of algebraic equations using Karash-Kuhn-Tucker (KKT) conditions so that we can reformulate the results analysis easily. By taking the KKT conditions of (9), we can obtain the following system of equations that are equivalent to equations (7) and (9), along with a restriction on $\boldsymbol{\beta}$ being within its approximate α % confidence region.

$$-2\nabla_r{}^2 P\Big|_{\hat{\mathbf{x}}_u^*}\left(\mathbf{x} - \mathbf{x}_\mathbf{u}^*\right) + \nabla_\mathbf{x}\mathbf{g}(\mathbf{x}, \boldsymbol{\beta})^T \boldsymbol{\mu} = \mathbf{0} \tag{10a}$$

$$\mathbf{g}(\mathbf{x}, \boldsymbol{\beta}) \leq \mathbf{0} \tag{10b}$$

$$\mu_i g_i(\mathbf{x}, \boldsymbol{\beta}) = 0 \tag{10c}$$

$$\mu_i \geq 0 \tag{10d}$$

$$\left(\boldsymbol{\beta} - \hat{\boldsymbol{\beta}}\right)^T \mathbf{Q}_\beta{}^{-1}\left(\boldsymbol{\beta} - \hat{\boldsymbol{\beta}}\right) \leq \chi^2(\alpha, \nu_\beta) \tag{10e}$$

$$\mathbf{x}_\mathbf{u}^* - \hat{\mathbf{x}}_\mathbf{u}^* = \frac{d\mathbf{x}_\mathbf{u}^*}{d\boldsymbol{\beta}}\left(\boldsymbol{\beta} - \hat{\boldsymbol{\beta}}\right) \tag{10f}$$

where i denotes the i^{th} inequality constraint. Equations (10e) and (10f) define the uncertainty of $\boldsymbol{\beta}$ and the unconstrained optimum, $\mathbf{x}_u^*$. Equations (10a) – (10d) defines the mapping which transforms the uncertainty of $\mathbf{x}_u^*$ in the reduced space to the uncertainty of $\mathbf{x}_c^*$ in the region defined by $\mathbf{g}(\mathbf{x}, \boldsymbol{\beta}) \leq \mathbf{0}$. Because of the change in the active set, the sensitivity matrix of $\mathbf{x}_c^*$ with respect to $\boldsymbol{\beta}$ (i.e. $\frac{d\mathbf{x}_c^*}{d\boldsymbol{\beta}}$) is not defined over the entire region of interest. The change in the active set is represented by the complementarity equation in (10c). Equations (10a) – (10f) describing the α% of confidence region of $\mathbf{x}_c^*$ will be used for results analysis in RTO systems.

3. RESULTS ANALYSIS IN REAL-TIME OPTIMIZATION

In this section, a new results analysis strategy to handle possible changes in the active set of inequality constraints is presented. The control structure has to be considered in results analysis. In this paper, we focus on the case in which the inequality constraints are the bounds on the decision variables, which are final elements or setpoints regulated by controllers at a much higher frequency than the RTO loop. In this situation, the inequality constraints are not a function of $\boldsymbol{\beta}$. Therefore, Equations (10a) – (10f) can be simplified further as follows

$$-2\nabla_r{}^2 P\Big|_{\hat{\mathbf{x}}_\mathbf{u}^*}\left(\mathbf{x}-\mathbf{x}_\mathbf{u}^*\right)+\nabla_\mathbf{x}\mathbf{g}(\mathbf{x})^T\boldsymbol{\mu}=\mathbf{0} \qquad (11a)$$

$$\mathbf{g}(\mathbf{x}) \le \mathbf{0} \qquad (11b)$$

$$\mu_i g_i(\mathbf{x}) = 0 \qquad (11c)$$

$$\mu_i \ge 0 \qquad (11d)$$

$$\left(\mathbf{x}_\mathbf{u}^*-\hat{\mathbf{x}}_\mathbf{u}^*\right)^T \mathbf{Q}_{\mathbf{x}_\mathbf{u}^*}{}^{-1}\left(\mathbf{x}_\mathbf{u}^*-\hat{\mathbf{x}}_\mathbf{u}^*\right) \le \chi^2(\alpha, \nu_X) \qquad (11e)$$

where (10e) and (10f) are combined to form (11e) and $\mathbf{Q}_{\mathbf{x}_\mathbf{u}^*}$ can be calculated from (4). Equations (11a) – (11e) defines the α% confidence region of the constrained optimum which will be used in results analysis.

The proposed strategy of results analysis compares the overlapping of two confidence regions of the optima predicted in successive RTO executions. The strategy is shown in Figure 3. The level of confidence, α%, that two confidence regions start overlapping is first estimated. If α is small ($\alpha \le \alpha_0$), we expect that large portions of 95% confidence regions of two uncertain optima overlap. Therefore, we conclude that the difference between two uncertain optima is due to common cause variability, and the new setpoint will not be implemented. If α is large ($\alpha > \alpha_0$), only small portions of 95% confidence regions overlap or two 95% confidence regions are even disjoint when α% is larger than 95%. We conclude that the new setpoint should be implemented, because the difference between two uncertain optima is due to non-stationary disturbances.

The confidence level, α%, at which two confidence regions just overlap can be determined by solving an optimization problem. When two confidence regions just overlap, there exists a value of $\mathbf{x}$ that satisfies the system of equations (11a) – (11e) for the last implemented and current RTO executions. Therefore, α can be calculated from the parameter, c, in (12).

$$\underset{\mathbf{x}}{\text{Minimize}}\ c \qquad (12)$$

Subject to

$$-2\nabla_r{}^2 P\Big|_{\hat{\mathbf{x}}_{\mathbf{u}j}^*}\left(\mathbf{x}-\mathbf{x}_{\mathbf{u}j}^*\right)+\nabla_\mathbf{x}\mathbf{g}(\mathbf{x})^T\boldsymbol{\mu}_j=\mathbf{0}$$

$$\mathbf{g}(\mathbf{x}) \le \mathbf{0}$$

$$\mu_{ij} g_i(\mathbf{x}) = 0$$

$$\mu_{ij} \ge 0$$

$$\left(\mathbf{x}_{\mathbf{u}j}^*-\hat{\mathbf{x}}_{\mathbf{u}j}^*\right)^T \mathbf{Q}_{\mathbf{x}_{\mathbf{u}j}^*}{}^{-1}\left(\mathbf{x}_{\mathbf{u}j}^*-\hat{\mathbf{x}}_{\mathbf{u}j}^*\right) \le c$$

and α can be found from the Chi-square distribution table as $c = \chi^2(\alpha, \nu_X)$. In (12), j = 1, 2 which denotes the previous and current RTO results. The value, α, is compared to a pre-specified value, α_0. If α is larger than α_0, the new setpoint will be implemented in the plant.

The parameter, α_0, is the tuning parameter for the results analysis for trading off variability and tracking. If α_0 is chosen to be 0%, results analysis will be turned off and all the variability will be transmitted to the plant. If α_0 is chosen to be 100%, there will be no variability, but the RTO system cannot track the changing optimum. Therefore, the designer has to choose a value of α between 0% and 100% to achieve an appropriate trade-off between tracking and variability.

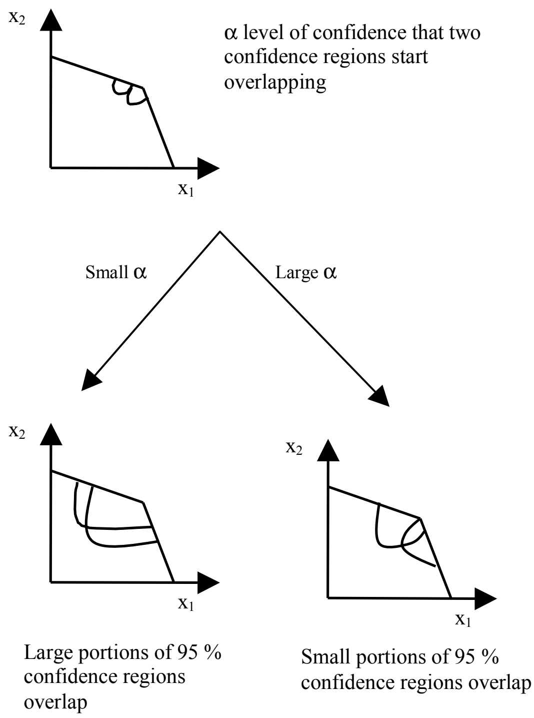

Fig. 3 Strategy of results analysis

The proposed results analysis strategy compares two approximate confidence regions linearized at the current and newly predicted optima. This strategy is appropriate when the current and newly predicted optima are "close" to each other, so that using linearized confidence regions for results analysis is a good approximation. In typical RTO applications, the plant model is optimized subject to a trust region to avoid a large plant movement in a single step. Since large plant moves are prevented in RTO, results analysis using linear confidence regions is appropriate.

4. WILLIAMS-OTTO REACTOR CASE STUDY

The proposed approach is applied to the simulated Williams-Otto reactor system described in Yip and Marlin (2002) as shown in Figure 4. It is assumed that there is no structural mismatch between the plant and the model used in RTO, but substantial parametric uncertainty exists. The optimization variables are the setpoint of the feed flow rate of B (F_b) and reactor temperature (T_r).

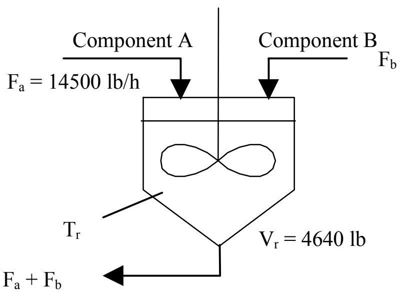

$A + B \rightarrow C \qquad k_1 = A_1 e^{-B_1/T_r}$

$C + B \rightarrow P + E \qquad k_2 = A_2 e^{-B_2/T_r}$

$P + C \rightarrow G \qquad k_3 = A_3 e^{-B_3/T_r}$

Fig. 4 Williams-Otto reactor system

The parameters selected for updating are the frequency factors, $\boldsymbol{\beta}^T = [A_1\ A_2\ A_3]$, using a single data set for updating. The measured variables are the reactor volume and temperature, feed flow rates of A and B, and all the compositions. Zero mean white noise is added to the process variables to simulate the measurement errors. The standard deviations for measurement noise are 1% for flows, 2% for reactor volume, 3% for composition and 3.3 R for temperature.

The inequality constraints in the optimizer are the maximum flow rate of feed B and the maximum allowable reactor temperature. There are no inequality constraints in model updating. Therefore, the covariance matrix for the estimated parameter in Equation (2) can be determined by linear sensitivity analysis. The confidence region of the optimizer results is determined from Equation (9) or Equations (11a) – (11e), where the covariance matrix of $\mathbf{x}_u^*$ is related to the covariance matrix of $\boldsymbol{\beta}$ by Equation (4). The approximate 95% confidence region for the constrained optimum gives a good approximation for the uncertain constrained optimum, as shown in Figure 5. Samples of $\boldsymbol{\beta}$ were used in the 500 Monte-Carlo nonlinear optimizations. The approximate 95% confidence region for the constrained $\mathbf{x}_c^*$ is bounded by solid lines on the constraints and the solid curve inside the feasible region. Most of the data points obtained from nonlinear optimizations are inside the approximated 95 % confidence region.

The performance of the RTO system with and without results analysis is shown in Figure 6. In this case study, 100 closed-loop RTO calculations were simulated and a 50% step increase in A_1 occurred at the 50^{th} RTO execution. Without results analysis, there are excessive plant movements due to the propagation of measurement noise. When the results analysis in (12) is implemented, unnecessary plant movements have been significantly reduced as shown in Figure 6.

The performance of the strategy for one value of the tuning parameter (α_0) is shown in Figure 6. When α_0 is equal to 50 %, an increase in total operating profit is achieved because of the reduction of the plant movements. Plant movements can further be reduced by choosing a larger value of α_0. However, the total profit achieved may be lower because the RTO system becomes less effective in profit tracking. When α_0 was chosen to be 0.7, the total profit achieved was \$106370, which was smaller than profit attained when there was no results analysis. Therefore, the designer has to trade off tracking and variability when tuning the results analysis.

The results analysis optimization problem in (12) may have multiple solutions because of the complementarity equations in the constraints, which are non-convex. We need to make sure that the solution of (12) is the global minimum for comparing with α_0. In the Williams-Otto reactor case study, after the value of α had been obtained, the α% confidence regions of two successive predicted optima were plotted to make sure that the solution was reasonable. This can be done because the optimization problem has a dimension of two. In large dimensional problem, we may need global optimization or re-formulation to obtain the global minimum of (12).

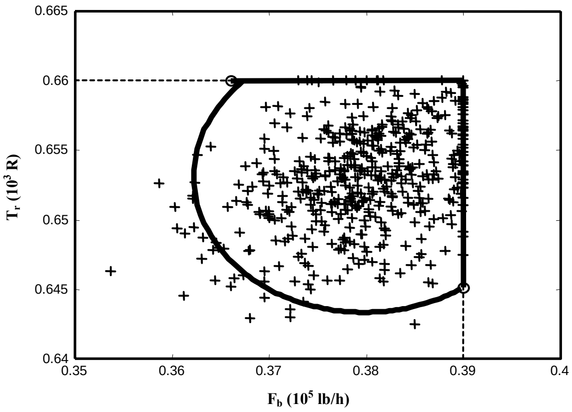

Fig. 5 Comparison of the approximated 95 % confidence region for the constrained optimum (bounded by solid lines on the constraints and solid curve inside the feasible region) with nonlinear optimization for sampled values of $\boldsymbol{\beta}$ (+).

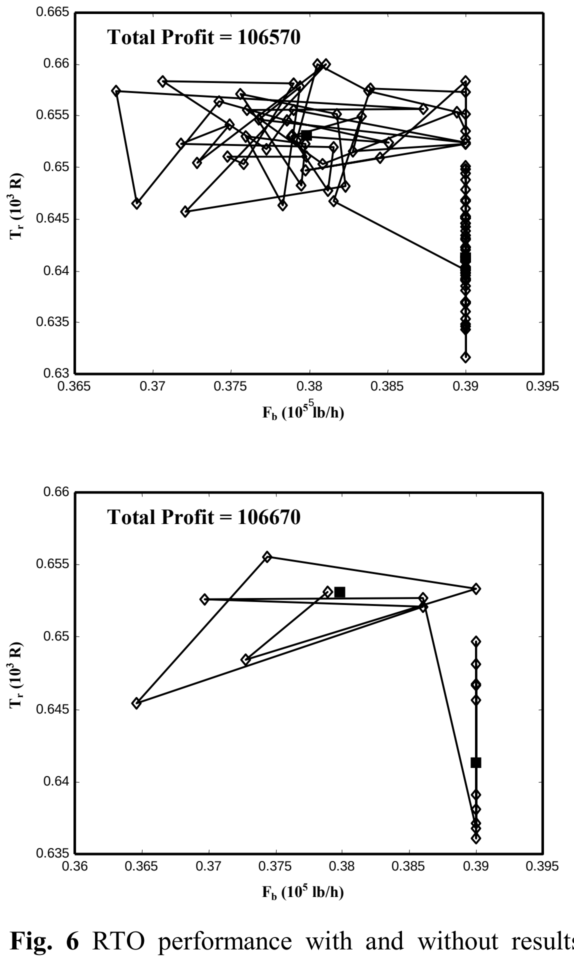

Fig. 6 RTO performance with and without results analysis for tracking the disturbance change of +50% change in A_1. Top: No results analysis, bottom: α_0 equal to 0.5. (◊ : setpoint implemented, ■ : true optimum before and after the disturbance)

5. CONCLUSIONS

A new results analysis strategy for a constrained RTO system has been proposed in this paper. The uncertainty of the constrained optimum, which represents the common cause variability, is determined by mapping the confidence region of the unconstrained optimum to feasible region. The mapping equations contain the complementarity equations, which model the change in the active set of inequality constraints for the anticipated uncertainty in the parameters. The mapping equations are used in the results analysis to compare two uncertain optima. The strategy of results analysis involves determining the level of confidence that two confidence regions start overlapping. The level of confidence is compared to a pre-specified value to determine if the optimizer result shall be implemented or not.

The proposed results analysis strategy has been successfully applied to the simulated Williams-Otto reactor case study. Plant movements responding to measurement noise have been significantly reduced and a higher operating profit can be achieved for a well-chosen tuning parameter.

6. REFERENCES

Anderson, T. W. (1984). *An Introduction to Multivariate Statistical Analysis*. Wiley, NY.

Fiacco, A. V. (1983). *Introduction to Sensitivity and Stability Analysis in Nonlinear Programming*. Academic Press, NY.

Marlin, T. E. and Hrymak, A. N. (1997). Real-Time Optimization of Continuous Processes. *Fifth International Conference on Chemical Process Control. AIChE Symp*., No. 316, 156, 1997.

Miletic, I. P. and Marlin, T. E. (1991). On-Line Statistical Results Analysis in Real-Time Operations Optimization. *Ind. Eng. Chem. Res*., 37, 3670-3684.

Ronholm, L and Marlin, T. E. (2002). Move Moderation in Real-Time Optimization. *ESCAPE-12*, The Hague, The Netherlands.

Wolbert, D., Joulia, X., Koehret, B., and Biegler, L. T. (1994). Flowsheet Optimization and Optimal Sensitivity Analysis Using Analytical Derivatives. *Comp. Chem. Eng.*, 18(11/12), 1083-1095.

Yip, W. S. and Marlin, T. E. (2002). Multiple Data Sets for Model Updating in Real-Time Operations Optimization. *Comp. Chem. Eng.* 26(10), 1345-1362.